

## $^{13}\text{C}$ NMR STUDIES OF *IN VIVO* KINETIC RATES OF METABOLIC PROCESSES†

J. A. DEN HOLLANDER and R. G. SHULMAN

Department of Molecular Biophysics and Biochemistry, Yale University, P.O. Box 6666,  
260 Whitney Avenue, New Haven, CT 06511, U.S.A.

(Received in USA 8 February 1983)

**Abstract**— $^{13}\text{C}$  NMR has been used to follow  $^{13}\text{C}$  labeling in suspensions of yeast cells, and in perfused mouse livers.

Using  $[1-^{13}\text{C}]$ glucose and  $[6-^{13}\text{C}]$ glucose label scrambling can be observed to occur during yeast glycolysis, both in fructose-1,6-diphosphate, and in trehalose. A quantitative analysis of the scrambling patterns allows one to obtain information about the kinetics of the aldolase/TPI triangle, and of futile cycling through PFK and through Fru-1,6-P<sub>2</sub>-ase. It is shown that the scrambling of the  $^{13}\text{C}$  label is different for aerobic and anaerobic glycolysis. This information can be used to study the effect of oxygen upon the kinetic rates of the TPI/aldolase part of the pathway.

Gluconeogenesis has been studied in yeast, using  $[2-^{13}\text{C}]$ acetate as a substrate, and in perfused mouse liver by using  $[3-^{13}\text{C}]$ alanine and  $[2-^{13}\text{C}]$ ethanol. The appearance of the label could be followed in aminoacids, intermediates, and in the end-product of gluconeogenesis. From the labeling patterns information is obtained about the flow of the label through the various pathways.

These experiments demonstrate that  $^{13}\text{C}$  NMR is a valuable technique to study the rate of metabolic processes *in vivo*.

Isotopic labeling has been used for a long time to quantitate metabolic pathways *in vivo*. An early application of this approach was the use of  $[1-^{14}\text{C}]$  and  $[6-^{14}\text{C}]$ glucose to determine the flow through the phosphogluconate pathway<sup>1-3</sup>. These experiments were based upon the fact that if  $[1-^{14}\text{C}]$ glucose enters this pathway  $^{14}\text{C}$  labeled  $\text{CO}_2$  will be formed, whereas the  $\text{CO}_2$  formed from  $[6-^{14}\text{C}]$  glucose will be unlabeled. In the glycolytic pathway the C<sub>1</sub> and C<sub>6</sub> carbons of glucose become indistinguishable below the triosephosphate isomerase (TPI) step, so that  $\text{CO}_2$  formed in the TCA cycle from both  $[1-^{14}\text{C}]$ glucose and  $[6-^{14}\text{C}]$ glucose will be equally labeled. Therefore, the difference in radioactivity in  $\text{CO}_2$  formed from  $[1-^{14}\text{C}]$  and  $[6-^{14}\text{C}]$ glucose provides a measure of the relative flux through the phosphogluconate pathway. An important application of these labeling techniques has been the study of gluconeogenesis in liver cells.<sup>4,5</sup> Here the appearance of the  $^{14}\text{C}$  label in the different carbons of glucose formed from  $^{14}\text{C}$  labeled substrates provides a measure of the disequilibrium of TPI, and of the contribution of the pentose shunt pathway.

The experiments to measure the phosphogluconate pathway involved the determination of radioactivity in  $\text{CO}_2$  formed, which is relatively straightforward. However, in general these experiments require tedious chemical procedures for the isolation and the breakdown of the metabolic end-product of interest, which has inhibited routine application of this experimental approach.

During the last several years  $^{13}\text{C}$  labeling has been applied increasingly. The availability of high-field NMR spectrometers, with a good sensitivity makes it feasible to utilize  $^{13}\text{C}$  NMR for these studies<sup>6-10</sup>.  $^{13}\text{C}$  NMR provides a very convenient method to determine the  $^{13}\text{C}$  label distribution in intermediates and in end-products of metabolic processes. Moreover,  $^{13}\text{C}$  NMR allows one to follow the  $^{13}\text{C}$  label in the intact biological system, thereby providing real-time information and avoiding possible artifacts of extraction

procedures. The possibility to measure simultaneously the timecourse of substrate utilization and of product formation together with information about label distributions in intermediates and products makes  $^{13}\text{C}$  NMR a powerful technique for these kind of studies. In addition, by using the  $^{13}\text{C}$ - $^{13}\text{C}$  splitting patterns in labeled compounds  $^{13}\text{C}$  NMR has the unique ability to obtain information about non-random label distributions. While that kind of information can be obtained from the intact system it is more conveniently obtained in extracts, which allows one to use long term data acquisitions under optimal conditions.

The most important disadvantage of the use of  $^{13}\text{C}$  NMR compared with  $^{14}\text{C}$  labeling techniques is its relative insensitivity. In modern NMR spectrometers a  $^{13}\text{C}$  NMR spectrum can be obtained from about 1  $\mu\text{mole}$  of a  $^{13}\text{C}$  labeled compound in a few minutes accumulation time. Smaller amounts of material require longer accumulations since the signal-to-noise ratio increases as the square root of the accumulation time. However, because of the increased interest in the application of stable isotopes,  $^{13}\text{C}$  labeled compounds are expected to become cheaper in the future. This will make it possible to increase the scope of  $^{13}\text{C}$  labeling experiments, extending these studies towards lower concentrations and to intact animals.<sup>11</sup>

In this paper we wish to discuss the results obtained by  $^{13}\text{C}$  NMR about carbohydrate metabolism. Examples discussed are taken from our studies of the *in vivo* rates of glycolytic enzymes in *Saccharomyces cerevisiae*, and the gluconeogenic pathway in liver and yeast.

*The aldolase/TPI triangle.* We have applied  $^{13}\text{C}$  NMR to study the glycolytic pathway in *Saccharomyces cerevisiae*.<sup>12,13</sup> For these studies we introduced  $[1-^{13}\text{C}]$  or  $[6-^{13}\text{C}]$ glucose into suspensions of yeast cells, and followed the metabolism of the labeled glucose in these suspensions by  $^{13}\text{C}$  NMR. Fig. 1 shows a typical  $^{13}\text{C}$  NMR spectrum, representing a 1 minute accumulation obtained about 10 min after the addition of  $[1-^{13}\text{C}]$ glucose up to 50 mM final concentration to a dense suspension of yeast cells. The yeast cells were obtained by harvesting them in

†This work was supported by National Institutes of Health Grant AM 27121.

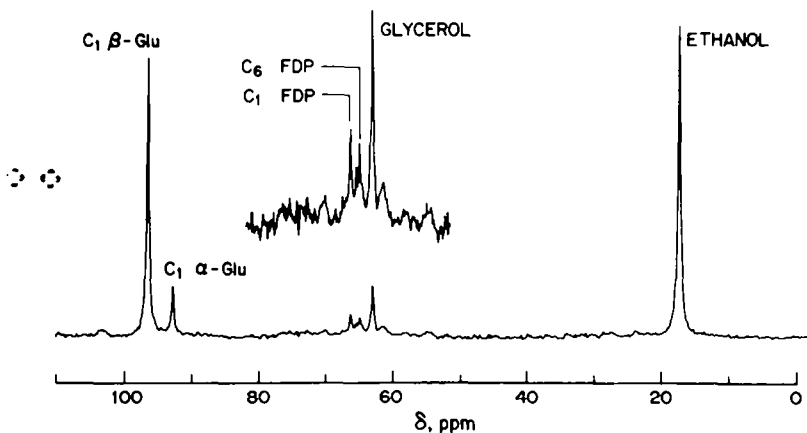


Fig. 1.  $^{13}\text{C}$  NMR Spectrum of a suspension of yeast cells, taken about 10 min after the addition of  $[1-^{13}\text{C}]$ glucose. The spectrum was obtained by accumulating 200 FID's in a total accumulation time of 1 min. Observed are the residual  $\text{C}_1$  signals of glucose,  $\text{C}_2$  of ethanol,  $\text{C}_1$  of glycerol, and  $\text{C}_1$  and  $\text{C}_6$  of the intermediate fructose-1,6-diphosphate.

the log-phase of growth in a rich medium with glucose as carbon source, so that they were glucose repressed at the beginning of the experiment. Broad band decoupling of protons was employed to obtain this spectrum. The signals at 93.0 and 96.8 ppm arise from the  $\text{C}_1$  carbon of  $\alpha$  and  $\beta$  glucose. It is clear from this spectrum that glucose was not in anomeric equilibrium while this spectrum was obtained, since in that case we would have expected the  $\alpha$  and  $\beta$  glucose peaks in a ratio of 2:3. Since glucose was in anomeric equilibrium at the moment glucose was added to the yeast suspension it is clear that the yeast cells have preferentially utilized the  $\alpha$  anomer. In fact, by following the time course of glucose utilization in a series of 1 minute  $^{13}\text{C}$  NMR spectra the utilization of glucose by yeast cells could be followed in detail. In this way we found that the ratio of the apparent Michaelis-Menten constants for  $\alpha$  and for  $\beta$  glucose utilization,  $K_{m\beta}/K_{m\alpha}$  is 1.8. Furthermore, we observe in the  $^{13}\text{C}$  NMR spectrum the signals of the  $\text{C}_2$  carbon of labeled ethanol (at 17.6 ppm), and of  $\text{C}_3$  of glycerol (63.3 ppm), the glycolytic end-products.

In addition to these substrate and end-products we were able to observe in this 1 min spectrum the signals of the intermediate fructose-1,6-bisphosphate (Fru-1,6- $\text{P}_2$ ). The spectrum shows that both the  $\text{C}_1$  (at 66.6 ppm) and the  $\text{C}_6$  carbons (65.4 ppm) of Fru-1,6- $\text{P}_2$  are labeled with  $^{13}\text{C}$ . We performed series of parallel experiments, using samples from the same batch of yeast cells, with  $[1-^{13}\text{C}]$  and  $[6-^{13}\text{C}]$ glucose. The results of these experiments are shown in Fig. 2. The upper trace of Fig. 2 shows the Fru-1,6- $\text{P}_2$  portion of a 5 minute  $^{13}\text{C}$  NMR spectrum, obtained during steady state glycolysis of  $[1-^{13}\text{C}]$ glucose in a suspension of glucose repressed yeast cells. The lower spectrum comes from a parallel experiment in which  $[6-^{13}\text{C}]$  glucose was used. The spectra show that in the experiment with  $[1-^{13}\text{C}]$ glucose Fru-1,6- $\text{P}_2$  is labeled both in the  $\text{C}_1$  and the  $\text{C}_6$  position. As expected the  $\text{C}_1$  signal is larger than the  $\text{C}_6$  signal; the ratio of  $\text{C}_6$  to  $\text{C}_1$  is measured to be 0.7. In the experiment with  $[6-^{13}\text{C}]$ glucose we find again that Fru-1,6- $\text{P}_2$  is labeled both in the  $\text{C}_6$  and the  $\text{C}_1$  position; here the ratio of  $\text{C}_1$  to  $\text{C}_6$  is measured to be 0.65.

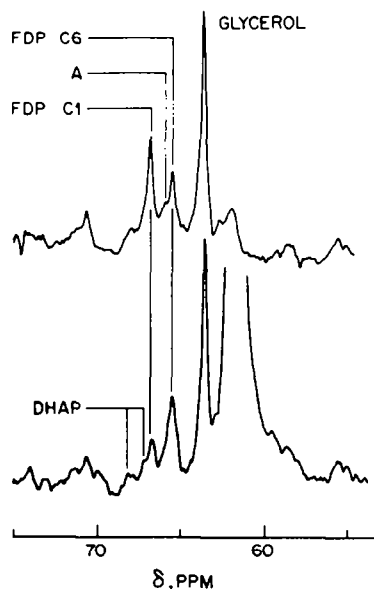


Fig. 2. Fructose-1,6-diphosphate region of the  $^{13}\text{C}$  NMR spectrum of yeast suspensions, which were fed either  $[1-^{13}\text{C}]$ glucose (upper spectrum), or  $[6-^{13}\text{C}]$ glucose (lower spectrum). Each spectrum represents a 5 min accumulation obtained during steady state glycolysis.

This "scrambling" of the label can be applied to determine the kinetics of the Fru-1,6- $\text{P}_2$  aldolase-TPI triangle. In order for the label to appear in  $\text{C}_6$  of Fru-1,6- $\text{P}_2$  starting from  $[1-^{13}\text{C}]$ glucose it is necessary that the label goes down the pathway to dihydroxyacetone phosphate (DHAP). From there the label appears in glyceraldehyde-3-phosphate (GAP). At that point there are 2 possibilities, depending upon the kinetics of this part of the pathway. If the rate of Fru-1,6- $\text{P}_2$  aldolase is relatively slow, then there will be only a small probability of the label reappearing in the  $\text{C}_6$  of Fru-1,6- $\text{P}_2$ . However, if the rate of aldolase is high the label can appear in the  $\text{C}_6$  position. Therefore, the "scrambling" of the label from the  $\text{C}_1$  to the  $\text{C}_6$  position reflects the kinetics of

aldolase. Similarly, the "scrambling" of the label from C<sub>6</sub> to C<sub>1</sub> in the [6-<sup>13</sup>C]glucose experiment depends both upon the rate of aldolase and of TPI. The [1-<sup>13</sup>C] and [6-<sup>13</sup>C]glucose experiments are complementary: the combination of these two experiments provides specific information about the rates of aldolase and of TPI.

We approached this problem by solving a kinetic scheme for this part of the pathway in the steady state situation, which relates the "scrambling" of the label for the two experiments to the relative forward and reverse rates through the two enzymes. The kinetic scheme used is shown in Fig. 3. Defining the ratio R<sub>16</sub> = (C<sub>6</sub>/C<sub>1</sub>) in Fru-1,6-P<sub>2</sub> in the [1-<sup>13</sup>C]glucose experiment, and R<sub>61</sub> = (C<sub>1</sub>/C<sub>6</sub>) in Fru-1,6-P<sub>2</sub> for the [6-<sup>13</sup>C]glucose experiment it can be shown that for the steady state solution of the kinetic scheme of Fig. 3 the relative unidirectional rates for TPI and for aldolase are related to R<sub>16</sub> and R<sub>61</sub> as follows:

$$\frac{\text{TPI}_{\text{backward}}}{\text{TPI}_{\text{forward}}} = \frac{k_4[\text{GAP}]}{k_3[\text{DHAP}]} = \frac{R_{61}(1 - R_{16})}{R_{16}(1 - R_{61})}$$

$$\frac{\text{Aldolase}_{\text{backward}}}{\text{Aldolase}_{\text{forward}}} = \frac{k_2[\text{GAP}][\text{DHAP}]}{k_1[\text{Fru-1,6-P}_2]} = \frac{2R_{61}}{R_{61} + \frac{R_{61}(1 - R_{16})}{R_{16}(1 - R_{61})}}$$

Therefore, from our measurements of R<sub>16</sub> = 0.7, and R<sub>61</sub> = 0.65, we can calculate TPI<sub>backward</sub>/TPI<sub>forward</sub> = 0.8, and aldolase<sub>backward</sub>/aldolase<sub>forward</sub> = 0.9. It follows that under these conditions both aldolase and TPI are close to being in equilibrium. It should be noted that in the present consideration possible contributions of the pentose shunt pathway to the "scrambling" in Fru-1,6-P<sub>2</sub> have been ignored. However, it can be demonstrated that including pentose shunt reactions will not appreciably change our conclusions about the TPI and aldolase reactions. This is because the

pentose shunt, and in particular the transaldolase reaction, does provide a way for the label to "scramble" from the C<sub>1</sub> position of Fru-1,6-P<sub>2</sub> to the C<sub>6</sub> position, but not the other way around. Therefore, inclusion of this reaction into our scheme only leads to the conclusion that TPI might even be closer to being in equilibrium than we derived while ignoring transaldolase.

We have used this approach to study the Pasteur Effect in *Saccharomyces cerevisiae*. In order to do these studies it was necessary to obtain respiratory competent yeast cells under well defined conditions. We approached this by growing the yeast cells using a medium with the weakly repressive carbohydrate raffinose as carbon source, and harvesting the cells in the log-phase of growth. Cells were resuspended to a density of 20% wet weight. Aerobic experiments were performed by bubbling a 95% O<sub>2</sub>/5% CO<sub>2</sub> gas mixture through a sample of the yeast suspension; anaerobic experiments were done on parallel samples from the same batch of yeast cells while bubbling 95% N<sub>2</sub>/5% CO<sub>2</sub> at the same rate. At the beginning of the experiments 75 mM [1-<sup>13</sup>C]glucose was added to the yeast suspensions, and perchloric acid extracts were taken about 10 min after glucose addition. It is known that the rate of glycolysis in respiratory competent yeast cells depends upon whether or not they are oxygenated. In agreement with earlier findings of Lynen<sup>14</sup> and of Stickland<sup>15</sup> we found, by <sup>13</sup>C NMR experiments that the rate of glucose utilization is reduced by about a factor 2 upon oxygenation. The label "scrambling" we have observed in Fru-1,6-P<sub>2</sub> allows us to study the effect of this changing glycolytic rate upon the relative kinetics of the aldolase/TPI triangle.

Figure 4 shows the <sup>13</sup>C NMR spectra which were obtained of extracts prepared of suspensions of derepressed yeast cells, during aerobic and anaerobic glycolysis of [1-<sup>13</sup>C]glucose. It is clearly seen from the spectra that there has been a "scrambling" of the <sup>13</sup>C label from C<sub>1</sub> to C<sub>6</sub> in Fru-1,6-P<sub>2</sub>, both during aerobic and anaerobic glycolysis. However, while the ratio of the C<sub>6</sub> to C<sub>1</sub> of Fru-1,6-P<sub>2</sub> is 0.84 during aerobic glycolysis, it is only 0.5 during anaerobic glycolysis. Furthermore, the spectra also show that the level of Fru-1,6-P<sub>2</sub> is very similar aerobically and anaerobically. The fact that the "scrambling" changes indicates that the kinetics of the aldolase/TPI triangle is being influenced by the presence of oxygen. From determinations of the glycolytic flow we know that the rate of glycolysis has been slowed down in aerobic conditions. The fact that the level of Fru-1,6-P<sub>6</sub> did not change much upon oxygenation indicates the existence of a control point in the lower part of the pathway, below GAP. This is confirmed by our observation of higher "scrambling" in aerobic conditions. If the apparent rate constant of GAP dehydrogenase has been reduced in aerobic conditions, there will be a higher probability that the label reappears in Fru-1,6-P<sub>2</sub> through aldolase activity; this is indeed what is observed.

*Futile cycling of phosphofructokinase/Fru-1,6-P<sub>2</sub>-ase.* *Saccharomyces cerevisiae* cells, when grown using a gluconeogenic carbon source such as ethanol or acetate will have an active Fru-1,6-P<sub>2</sub>-ase. When such cells are exposed to glucose this enzyme will be inactivated over the period of about one

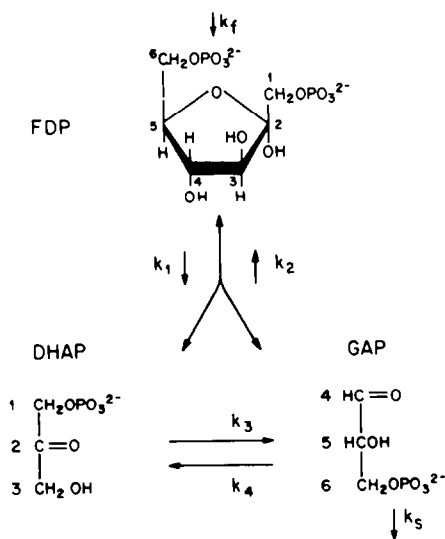


Fig. 3. Kinetic scheme of the fructose-1,6-diphosphate aldolase/triosephosphate isomerase part of the glycolytic pathway. The scheme illustrates the scrambling of the <sup>13</sup>C label between C<sub>1</sub> and C<sub>6</sub> in fructose-1,6-diphosphate.

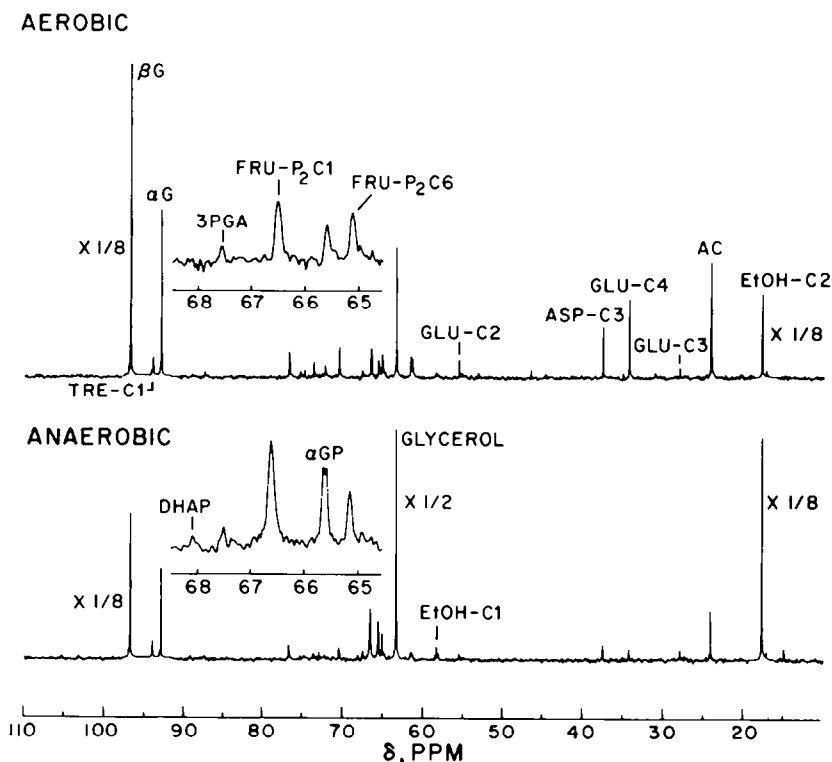


Fig. 4.  $^{13}\text{C}$  NMR Spectra of extracts taken during aerobic and anaerobic glycolysis of  $[1-^{13}\text{C}]$ glucose. The insets show the fructose-1,6-diphosphate part of the spectrum, to illustrate that the  $\text{C}_6/\text{C}_1$  ratio is higher during aerobic glycolysis than it is during anaerobic glycolysis. The amount of label which has appeared in the aminoacids glutamate (GLU) and aspartate (ASP) is higher in aerobic than in anaerobic glycolysis, reflecting more flow into the TCA cycle.

hour.<sup>16,17</sup> However, during this initial period the yeast cells contain both the enzymes phosphofruktokinase, and Fru-1,6- $\text{P}_2$ -ase. It is interesting to note that under the experimental conditions of Pasteur Effect both enzymes are usually present, since for those experiments it is necessary to utilize derepressed cells. Therefore, to understand the molecular basis of the Pasteur Effect one has to consider the effect of possible futile cycling of these two enzymes.

We obtained yeast cells, grown with acetate as carbon source, and used these cells to study aerobic and anaerobic glycolysis.  $[1-^{13}\text{C}]$ glucose was added to an aerobic suspension of these yeast cells, and an extract was prepared after the exhaustion of the  $^{13}\text{C}$  labeled glucose. A parallel experiment was performed using  $[6-^{13}\text{C}]$ glucose instead.  $^{13}\text{C}$  NMR spectra were measured of the extracts thus prepared.

The upper trace of Fig. 5 shows the  $^{13}\text{C}$  NMR spectrum of an extract which was prepared after utilization of  $[1-^{13}\text{C}]$ glucose. The spectrum shows, as expected, the appearance of the  $^{13}\text{C}$  label in ethanol, and in the aminoacids glutamate and aspartate. In addition to these products we also observe that the label has appeared in the  $\text{C}_1$  position of the storage carbohydrate, trehalose. The  $\text{C}_1$  signal of trehalose is much more intense than the signals from the  $\text{C}_2$ ,  $\text{C}_3$ ,  $\text{C}_4$  and  $\text{C}_5$  carbons. This shows that trehalose has been formed from the labeled glucose. In addition to the  $\text{C}_1$  signal the signal from the  $\text{C}_6$  carbon is also much more intense than the other carbons. Therefore, not only  $\text{C}_1$  has been enriched with  $^{13}\text{C}$ , but  $\text{C}_6$  has also been enriched. Correcting for the natural

abundance background (using the intensities of the unlabeled carbons of trehalose) we find that the relative intensity of  $\text{C}_6$  to the  $\text{C}_1$  of trehalose to be 0.22.

The trehalose synthesizing pathway in yeast starts with the intermediate glucose-6-phosphate (G6P).<sup>18</sup> Therefore, the labeling pattern in trehalose can be considered to reflect the label distribution in G6P during glycolysis of the  $^{13}\text{C}$  labeled glucose. The label distribution in G6P in this period was not observed however, because of overlap with the peaks from  $[1-^{13}\text{C}]$ glucose. There is more than one mechanism which might contribute to the "scrambling" of the label in G6P. We have already seen that there is a corresponding labeling pattern in Fru-1,6- $\text{P}_2$ . Therefore, the most straightforward explanation of the labeling pattern in G6P is that under the present conditions the enzyme Fru-1,6- $\text{P}_2$ -ase has been active; in that way the "scrambling" of the label we have observed previously in Fru-1,6- $\text{P}_2$  can reappear in fructose-6-phosphate (F6P), and then by the phosphoglucosomerase reaction in G6P. The other possibility would be that the pentose cycle enzyme, transaldolase would be responsible for the reappearance of the label in the  $\text{C}_6$  position of F6P. This explanation of "scrambling" of the label in G6P does not seem to be very likely in view of the fact that we have already established that this pathway did not contribute appreciably to the "scrambling" in Fru-1,6- $\text{P}_2$ .

The uncertainty about the origin of the labeling pattern in trehalose can be resolved as before by performing a parallel experiment with  $[6-^{13}\text{C}]$ glucose.

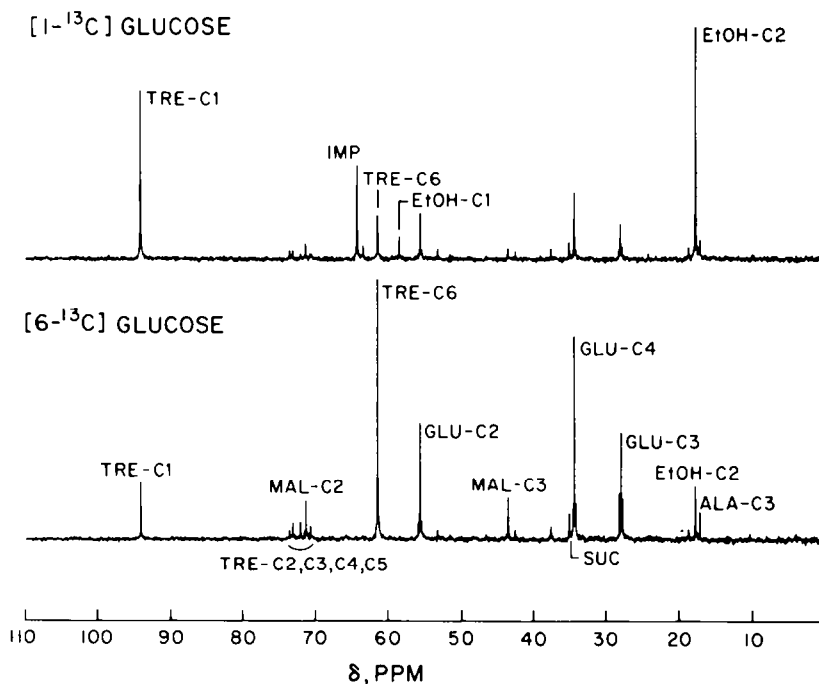


Fig. 5. <sup>13</sup>C NMR Spectra of perchloric acid extracts of aerobic suspensions of yeast cells prepared after the utilization of [1-<sup>13</sup>C]glucose (top spectrum) and of [6-<sup>13</sup>C]glucose (bottom spectrum). Spectra were collected with 2 s pulse intervals, with a total of 2500 accumulations. In the two spectra trehalose is seen to be labeled in both the C<sub>1</sub> and the C<sub>6</sub> positions. Glu-C4, Glu-C2, Glu-C3, glutamate-C<sub>4</sub>, -C<sub>2</sub> and C<sub>3</sub>; tre, trehalose; ala-C3, alanine-C<sub>3</sub>; EtOH-C1, EtOH-C2, ethanol-C<sub>1</sub>, -C<sub>2</sub>; mal-C2, mal-C3, malate-C<sub>2</sub>, -C<sub>3</sub>; imp, impurity.

The result of that experiment is shown in the lower trace of Fig. 5. Here it is seen that not only the C<sub>6</sub> of trehalose is enriched with <sup>13</sup>C, but also the C<sub>1</sub>. The ratio of C<sub>1</sub> to C<sub>6</sub> of trehalose, as determined in this experiment is found to be 0.20. This is indeed nearly the same as the corresponding ratio in the [1-<sup>13</sup>C]glucose experiment, which confirms that the transaldolase pathway makes only a minor contribution to the scrambling observed in G6P. Therefore, the scrambling of the label observed in trehalose depends upon Fru-1,6-P<sub>2</sub>-ase activity, and can actually be used to determine the relative flows through PFK and through Fru-1,6-P<sub>2</sub>-ase.

In order to make a quantitative determination of the flow through Fru-1,6-P<sub>2</sub>-ase consider a kinetic scheme which includes glucose phosphorylation, trehalose synthesis (from glucose-6-phosphate), phosphoglucoisomerase (assumed to be rapid), PFK, and Fru-1,6-P<sub>2</sub>-ase. This kinetic scheme can be solved for the steady state condition, which gives the following result:

$$\frac{v}{v'} = f_1 \left[ \frac{1}{r_{61}} - \frac{1}{R_{61}} \right]$$

where *v* is the rate of glucose phosphorylation, *v'* is the rate of Fru-1,6-P<sub>2</sub>-ase, and *f*<sub>1</sub> is the fraction labeled of the Fru-1,6-P<sub>2</sub>-C<sub>1</sub> carbon during the experiment with [6-<sup>13</sup>C]glucose. In this expression R<sub>61</sub> is defined as the ratio of C<sub>6</sub> to C<sub>1</sub> in Fru-1,6-P<sub>2</sub>, and r<sub>61</sub> is the corresponding ratio for trehalose. From the observations presented here it follows that 1/r<sub>61</sub> = 5.9; in a separate experiment we found that under the present conditions the "scrambling" in Fru-1,6-P<sub>2</sub> is

close to being complete (data not presented), from which it follows that R<sub>61</sub> = 1, and *f*<sub>1</sub> = 0.5. Using these numbers we deduce that *v'* = 0.44 *v*. From the <sup>13</sup>C NMR spectra versus time of the cellular suspension we estimate that 25% of the glucose ends up in the storage products trehalose and glycogen. From this we estimate that the flow through Fru-1,6-P<sub>2</sub>-ase is 37% of that through PFK. We therefore conclude that under these particular conditions there is a substantial amount of futile cycling. This cycling will enhance any control expressed at PFK in aerobic glycolysis and should therefore be taken into account in discussions of the Pasteur Effect.

We note, in passing, that the same cells under anaerobic conditions have been shown by saturation transfer measurements to have a negligible amount of futile cycling (Alger, Campbell, den Hollander and Shulman, to be published).

*The TCA and the glyoxylate cycle in yeast.* Intermediates of the TCA cycle can be labeled very efficiently by introducing <sup>13</sup>C labeled acetate into aerobic suspensions of yeast cells.<sup>19,20</sup> There are two possible pathways for labeled acetate to enter into the metabolic pools of yeast: one is by way of the TCA cycle, and the other is through the glyoxylate cycle.<sup>21</sup> The labeling patterns expected for intermediates and products are expected to be different for the two pathways. If [2-<sup>13</sup>C]acetate enters through the glyoxylate cycle we expect the intermediate oxaloacetate to become labeled in the C<sub>2</sub> and C<sub>3</sub> carbons, whereas the carboxyl carbons are expected to remain unlabeled. However, if [2-<sup>13</sup>C]acetate enters through the TCA cycle we expect a different labeling pattern for oxaloacetate. After several turns of the

TCA cycle we expect oxaloacetate to become labeled at the  $C_2$  and  $C_3$  carbons, whereas the enrichment expected for the carboxyl carbons will increase towards 50%. Oxaloacetate is an intermediate of low concentration, and not readily observed by  $^{13}\text{C}$  NMR. However, oxaloacetate can be considered to be substrate for gluconeogenesis, and also for the formation of aspartate. Therefore, the labeling pattern in oxaloacetate is reflected in these products of metabolism.

Figure 6 gives the  $^{13}\text{C}$  NMR spectra obtained of a suspension of yeast cells, after the introduction of  $[2-^{13}\text{C}]$ acetate. For this experiment the cells were grown in a medium with acetate as a carbon source, and resuspended to a density of 20% wet weight. The cells were oxygenated by bubbling oxygen through the suspension, and the  $^{13}\text{C}$  NMR spectra obtained by accumulation for 4 min periods, starting immediately after the addition of the labeled acetate. The spectra of Fig. 6 show the appearance of the  $^{13}\text{C}$  label in the aminoacids aspartate and glutamate, and in the storage carbohydrate, trehalose. The splitting patterns observed in these spectra are due to isotropic  $^{13}\text{C}$ - $^{13}\text{C}$  spin-spin couplings. In the upper

spectrum the  $C_4$  of glutamate appears at a singlet, reflecting the fact that the  $^{13}\text{C}$  label has appeared in  $C_4$  of glutamate while the neighboring  $C_3$  carbons of glutamate are not yet labeled. The initial appearance of the label in  $C_4$  of glutamate is in accord it being derived from the TCA-cycle intermediate  $\alpha$ -ketoglutarate, which was directly labeled from the entry of  $^{13}\text{C}$  labeled acetyl-CoA into the TCA cycle. In time we observe the appearance of a doublet in the  $C_4$  region of glutamate, in addition to the originally observed singlet. This doublet is due to glutamate, doubly labeled in the  $C_4$  and the  $C_3$  carbons. The series of spectra show that in time singly labeled glutamate is being replaced by multiply labeled glutamate; this observation indicates that glutamate is continuously being turned over and in time becomes highly labeled in the  $C_2$ ,  $C_3$  and  $C_4$  carbons.

Under the present conditions we observe the formation of the storage carbohydrate trehalose. Trehalose is an end-product of gluconeogenesis in yeast. From  $^{13}\text{C}$  NMR taken of extracts prepared of these yeast cells we found that the trehalose is highly and equally labeled at the  $C_1$ ,  $C_2$ ,  $C_5$  and  $C_6$

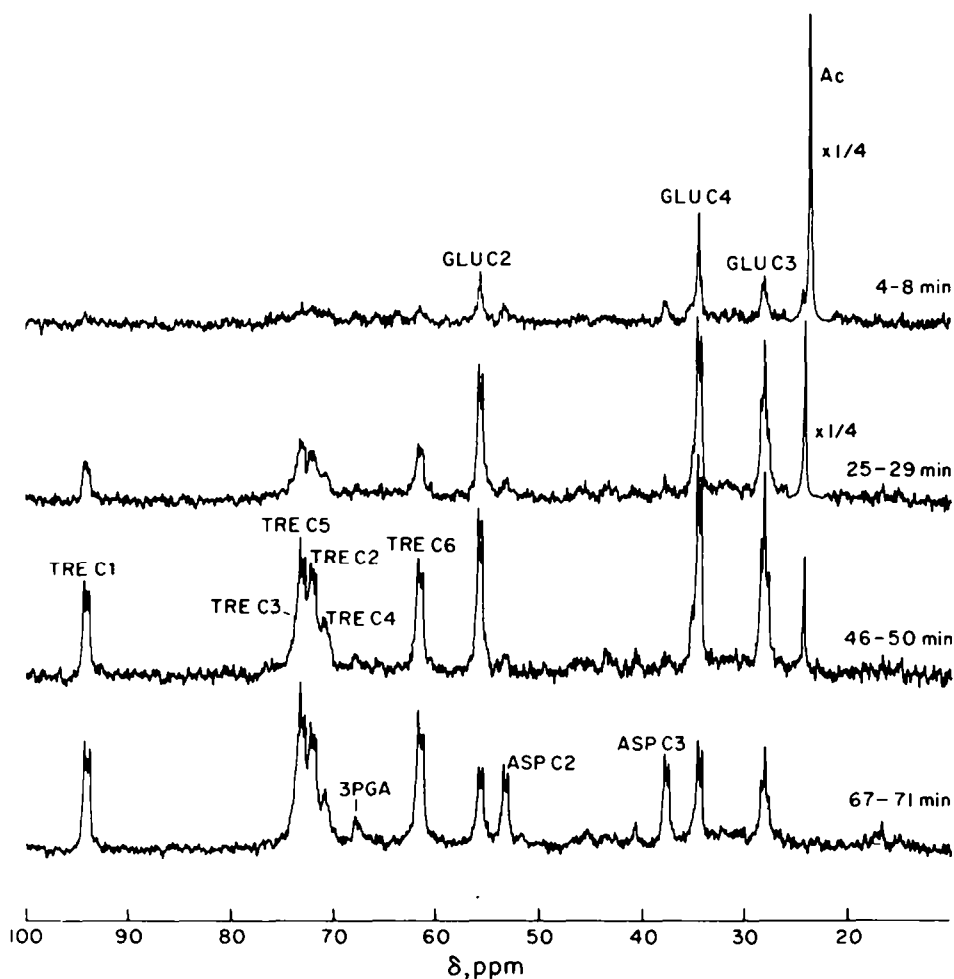


Fig. 6. Series of  $^{13}\text{C}$  NMR spectra of an aerobic suspension of yeast cells (20% wet weight). At time zero 100 mM  $[2-^{13}\text{C}]$ acetate was added to the suspension, after which  $^{13}\text{C}$  NMR spectra were collected in 250 s. blocks. Pulse intervals used were 0.5 s. The first peaks to appear are due to glutamate (GLU); these are followed by trehalose (TRE), and after acetate exhaustion, aspartate (ASP).

positions, whereas labeling of the  $\text{C}_3$  and  $\text{C}_4$  carbons is about 3 times lower. This shows that oxaloacetate (from which trehalose can be thought to be synthesized through gluconeogenesis) was highly enriched in the  $\text{C}_2$  and  $\text{C}_3$  carbons, while the enrichment of the carboxyl carbons was 3 times lower. From our previous argument that oxaloacetate as formed by the glyoxylate cycle remains unlabeled in the carboxyl carbons, whereas oxaloacetate coming from the TCA cycle is labeled up to 50% in the carboxyl carbons we infer that the TCA cycle and the glyoxylate cycle contribute about equally to the oxaloacetate used for gluconeogenesis.

These three examples from yeast metabolism show that the "scrambling" of the label which we observed under various conditions in Fru-1,6-P<sub>2</sub> in trehalose formed from labeled glucose, and in trehalose formed from acetate all give specific kinetic information about *in vivo* metabolic processes.

**Gluconeogenesis in perfused mouse liver** The  $^{13}\text{C}$  labeling method has been used to follow gluconeogenesis in liver cells and in perfused mouse livers. Labeled substrates have been used—at different times studies have been made with  $^{13}\text{C}$  labeled glycerol,<sup>22</sup> lactate,<sup>25</sup> alanine<sup>23-26</sup> and ethanol.<sup>24,25</sup> We shall discuss the experiments starting from labeled alanine and ethanol, in order to show the kinds of information that can be obtained from these studies.

Figure 7 shows the  $^{13}\text{C}$  NMR spectra of perfused mouse liver before and after the introduction of [3- $^{13}\text{C}$ ]alanine and unlabeled ethanol. The background peaks from the natural abundance  $^{13}\text{C}$  (1.1% abundant) in fatty acids are seen in the lower spectrum. The upper spectrum shows the  $^{13}\text{C}$  NMR

spectrum accumulated between 150 and 180 min after the substrates were introduced. This spectrum was taken in 30 min, however it is clear that by sacrificing some signal-to-noise the concentrations of metabolites corresponding to the different peaks can be measured more often. Several interesting features of this spectrum are immediately apparent. First, the six carbons of the glucose synthesized are labeled, but not equally.  $\text{C}_1$ ,  $\text{C}_2$ ,  $\text{C}_5$  and  $\text{C}_6$  are strongly labeled, while  $\text{C}_3$  and  $\text{C}_4$  are only weakly labeled. Second, intermediates of the pathway are observed to be labeled. In particular the amino acids glutamate and aspartate are labeled, as well as glutamine and alanine  $\text{C}_2$ . Note that  $\text{C}_2$ ,  $\text{C}_3$  and  $\text{C}_4$  of glutamate are all labeled but that the  $\text{C}_4$  labeling is low compared to the other two sites. Glutamate  $\text{C}_4$  will be labeled by the labeled alanine which has entered the TCA cycle via acetyl CoA while the  $\text{C}_2$  and  $\text{C}_3$  labeling comes from the flow from alanine to oxaloacetate (OAA) via the anaplerotic pathway and from succinate by way of the TCA cycle. Third, a peak has been observed from the alanine  $\text{C}_2$  position (the  $\alpha$ -C), which grows with time. Since alanine was originally labeled at  $\text{C}_3$  (the Me group) it has been possible to show that the  $\text{C}_2$  peak is a measure of the biosynthesis of new alanine from PEP, through pyruvate kinase. The new peak appears because in oxaloacetate the original label has been "scrambled" because of fumarase activity. Hence the PEP formed from oxaloacetate has some labeling at its  $\text{C}_3$  position (corresponding to the original  $\text{C}_3$  label of alanine) and some labeling at its  $\text{C}_2$  position (coming from the scrambling). The label distribution at PEP cannot be determined by direct observation of the PEP resonances, presumably because its concentration is too

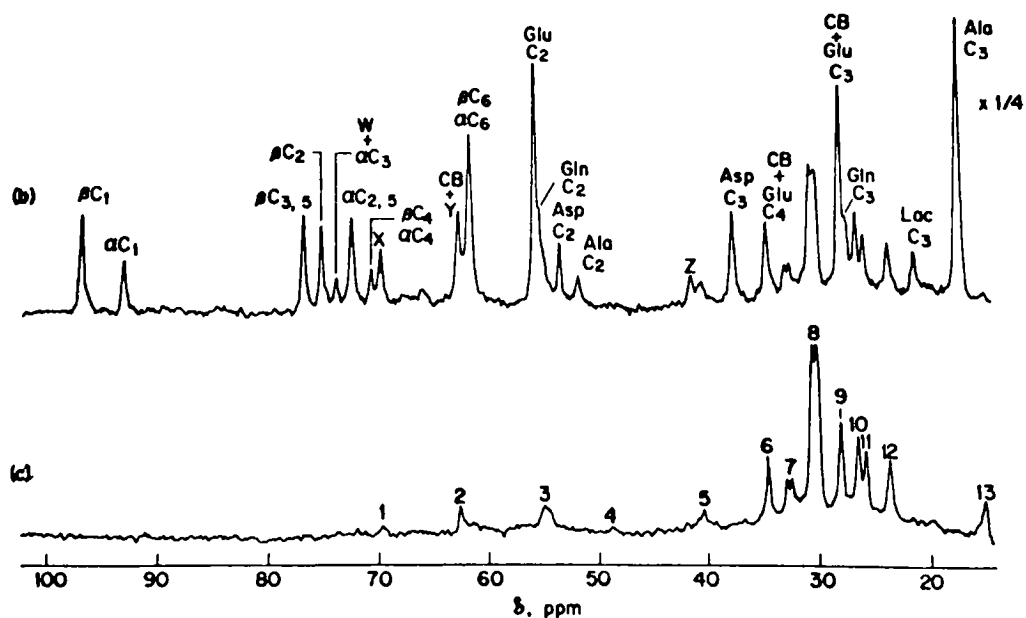


Fig. 7.  $^{13}\text{C}$  NMR Spectra from a perfused mouse liver at 35°. (c)  $^{13}\text{C}$  natural abundance background of this liver, accumulated before the substrate was added. The substrate, 8 mM [3- $^{13}\text{C}$ ]alanine and 20 mM unlabeled ethanol, was then added at 0 min and again at 120 min, and a series of  $^{13}\text{C}$  NMR spectra were taken. (b) Spectrum measured during the period 150–180 min. The pulse repetition time was 0.5 sec. The abbreviations used include:  $\beta\text{C}_1$ ,  $\alpha\text{C}_1$ ,  $\beta\text{C}_{3,5}$ ,  $\beta\text{C}_2$ ,  $\alpha\text{C}_3$ ,  $\alpha\text{C}_{2,5}$ ,  $\alpha\text{C}_4$ ,  $\beta\text{C}_6$  and  $\alpha\text{C}_6$ , the carbons of the glucose anomers; Glu C<sub>2</sub>, glutamate C<sub>2</sub>; Gln C<sub>2</sub>, glutamine C<sub>2</sub>; Asp C<sub>2</sub>, aspartate C<sub>2</sub>; Ala C<sub>2</sub>, alanine C<sub>2</sub>; Lac C<sub>3</sub>, lactate C<sub>3</sub>; CB, cell background peak; W, X, Y, Z, unknowns.

low. It can however, be inferred, with considerable certainty, from the label distribution observed in glucose, formed from PEP. From this it is possible to calculate the flow through pyruvate kinase, and to see how this flow is altered by different conditions.

The competition between alanine and ethanol can be followed from this kind of NMR measurement. Results have been reported about this competition in both hepatocytes and perfused liver, both of which we discuss, showing how similarly the two preparations behave. Figure 8 compares the spectra of perfused mouse livers with  $[3-^{13}\text{C}]$ alanine and with unlabeled ethanol (top spectrum) and with labeled  $[2-^{13}\text{C}]$ ethanol (bottom). The glucose labeling is very similar in the two spectra, and closely resembles the pattern seen when labeled alanine alone was present (data not shown), i.e.  $\text{C}_3$  and  $\text{C}_4$  are weakly labeled relative to the other four sites. The main difference between Figs. 8(a) and 8(b) is the absence of labeled amino acids in the spectrum of Fig. 8a. The labeled glutamate and aspartate peaks do appear in the spectrum of Fig. 8b, where labeled ethanol was used. It can be shown from these results that in the presence of ethanol alanine is almost completely confined to the anaplerotic path, entering as OAA, while ethanol dominates the acetyl CoA pathway. In other studies on the perfused liver (not shown), where alanine alone was the substrate, it has been observed that alanine flows almost equally through the two pathways into the TCA cycle.

In hepatocyte suspensions a more complete study of the ethanol and alanine competition has been reported<sup>23</sup> and Fig. 9(a) shows the results of feeding alanine alone. There are approximately equal concentrations of the  $^{13}\text{C}$  label at  $\text{C}_2$ ,  $\text{C}_3$  and  $\text{C}_4$  of glutamate

showing that both paths into the TCA cycle are taken by alanine. In Fig. 9(b) the competition between alanine and unlabeled ethanol causes a decrease in the ketone body peaks (from acetoacetate  $\text{C}_2$ ) and also eliminates the glutamate  $\text{C}_4$  peak—all of which is consistent with unlabeled ethanol having reduced the flow of alanine into the acetyl CoA pathway. It has been mentioned that two well known control mechanisms are expected to work in a complementary way to cause this flux change. First the increased mitochondrial ratios of  $\text{NADH}:\text{NAD}^+$  and acetyl-CoA:CoA brought about by ethanol both serve to convert the pyruvate dehydrogenase complex to its inactive form<sup>27</sup> thereby inhibiting further formation of acetyl CoA from pyruvate. Second, in a complementary way, acetyl CoA will activate pyruvate carboxylase<sup>28</sup> thereby increasing the flux into oxaloacetate. Returning to Fig. 9 trace c and d show the results obtained with labeled ethanol and labeled alanine (c) and with labeled ethanol and unlabeled alanine (d). The last spectrum shows very directly the metabolism of ethanol by the hepatocytes. The acetate formed from ethanol is present at high concentrations, as well as the ketone bodies  $\beta$  hydroxybutyrate ( $\beta$ -HB) and acetoacetate (AA) which are formed from acetyl CoA. Glutamate  $\text{C}_4$  is strongly labeled, as expected by its formation through the TCA cycle from acetyl CoA, while Glu  $\text{C}_2$  and  $\text{C}_3$  peaks are weakly labeled compared to Fig. 9(c), where the alanine has labeled them almost as strongly as ethanol has labeled  $\text{C}_4$ . The label distribution in glucose is very similar in all four spectra of Fig. 9. It shows high labeling at  $\text{C}_1$ ,  $\text{C}_2$ ,  $\text{C}_5$  and  $\text{C}_6$  and much lower labeling at  $\text{C}_3$  and  $\text{C}_4$ . The lower  $\text{C}_3$  and  $\text{C}_4$  intensities reflect that labeling of these carbons

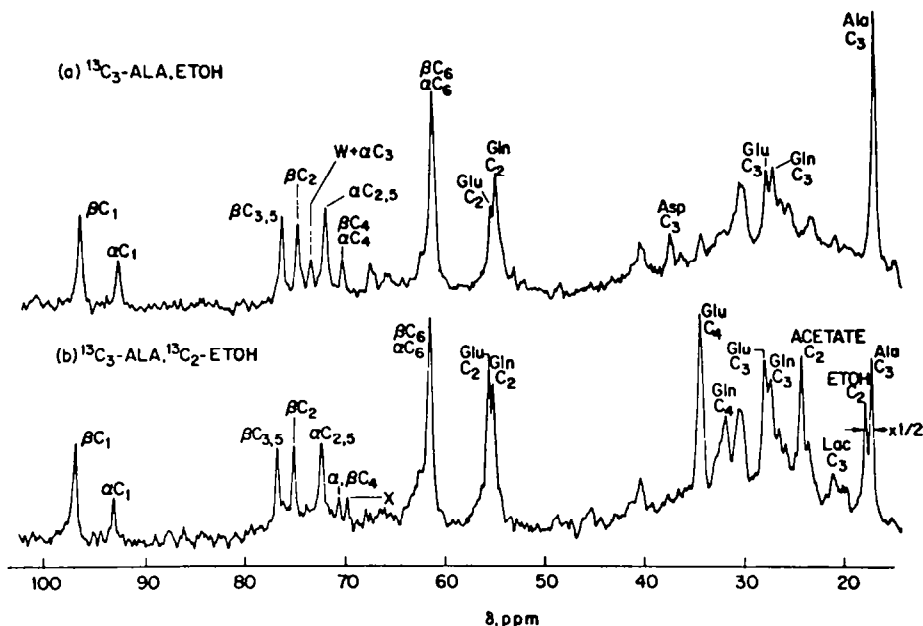


Fig. 8.  $^{13}\text{C}$  NMR Spectra of perfused mouse livers at  $35^\circ$ . Spectrum (a) is part of a sequence and was accumulated during the period 90–120 min. The substrate, here 8 mM  $[3-^{13}\text{C}]$ alanine and 8 mM unlabeled ethanol, was added at 0 min and again at 90 min. Spectrum (b), which also covers the period 90–120 min, was taken from a similar series of spectra taken of another perfused mouse liver; this liver was treated exactly the same as the liver shown in (a); however in this sequence the substrate was 8 mM  $[3-^{13}\text{C}]$ alanine and 8 mM  $[2-^{13}\text{C}]$ ethanol.



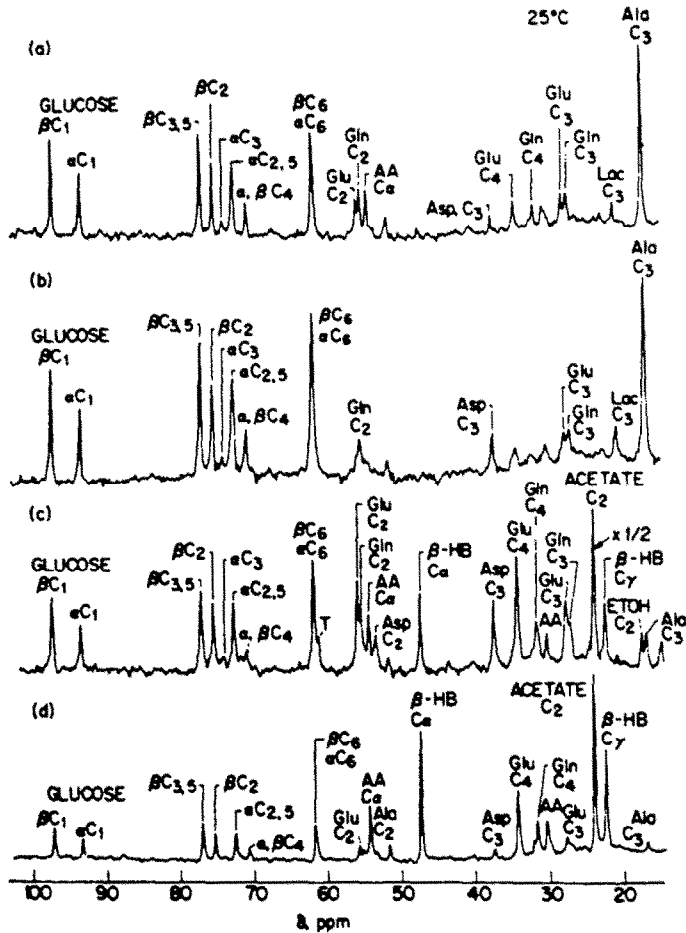


Fig. 9.  $^{13}\text{C}$  NMR Spectra at  $25^\circ$  of hepatocytes from euthyroid rats. One spectrum from a sequence is shown for each of four different cell samples. Substrates are: (a)  $[3\text{-}^{13}\text{C}]$ alanine; (b)  $[3\text{-}^{13}\text{C}]$ alanine and unlabeled ethanol; (c)  $[3\text{-}^{13}\text{C}]$ alanine and  $[2\text{-}^{13}\text{C}]$ ethanol; and (d) unlabeled alanine and  $[2\text{-}^{13}\text{C}]$ ethanol. Each spectrum was taken 145–175 min after addition of substrate. Alanine was administered at 28 mM and ethanol at 20 mM. AAC<sub>3</sub>, acetoacetate C<sub>2</sub>;  $\beta$ -HB C<sub>4</sub>, D- $\beta$ -hydroxybutyrate C<sub>2</sub>;  $\beta$ -HB C<sub>7</sub>, D- $\beta$ -hydroxybutyrate C<sub>4</sub>, ETOH C<sub>2</sub>, ethanol CH<sub>3</sub>; T is due to the buffer, and AA is acetoacetate C<sub>4</sub>.

depends upon additional turning of the TCA cycle, in which glutamate C<sub>2</sub> and C<sub>3</sub> become C<sub>1</sub> and C<sub>4</sub> of OAA. Since C<sub>5</sub> of glutamate is not directly labeled, labeling in these carbons of OAA comes only from C<sub>2</sub> of glutamate. Labeling at C<sub>3</sub> and C<sub>4</sub> of glucose is lowered if the C<sub>2</sub> of glutamate is not strongly labeled, as is the case in Fig. 9(d) where only labeled ethanol was introduced. This is consistent with the very weak C<sub>3</sub> and C<sub>4</sub> glucose peaks observed.

Hence it is clear from these illustrations that the label from ethanol is distributed amongst the intermediates of the TCA cycle and that the flow of the label from ethanol into glucose can be followed directly by  $^{13}\text{C}$  NMR.

#### REFERENCES

- B. Bloom and D. Stetten, Jr., *J. Am. Chem. Soc.* **75** 5446 (1953).
- B. Bloom, M. R. Stetten and D. Stetten, Jr., *J. Biol. Chem.* **204** 681 (1953).
- H. Beevers, M. Gibbs, *Nature* **173** 640 (1954).
- H. G. Wood, J. Katz and B. L. Landau, *Biochem. Z.* **338**, 809 (1963).
- J. Katz and R. Rognstad, *Trends Biochem. Sci.* **3**, 171 (1978).
- N. A. Matwyoff, and D. G. Ott, *Science* **181**, 1125 (1973).
- R. G. Shulman, T. R. Brown, K. Ugurbil, S. Ogawa, S. M. Cohen and J. A. den Hollander, *Science* (Washington, D.C.), **205**(4406), 160 (1979).
- K. Ugurbil, R. G. Shulman and T. R. Brown, High resolution  $^{31}\text{P}$  and  $^{13}\text{C}$  nuclear magnetic resonance studies of *Escherichia coli* cells *in vivo*. In *Biological Applications of Magnetic Resonance* (Edited by R. G. Shulman). Academic Press, New York (1979).
- R. S. Norton, *Bull. Mag. Res.* **3**, 29 (1980).
- A. I. Scott and R. L. Baxter, *Ann. Rev. Biophys. Bioengng* **10**, 151 (1981).
- J. R. Alger, L. O. Sillerud, K. L. Behar, R. J. Gillies, R. G. Shulman, R. E. Gordon, D. Shaw and P. E. Hanley, *Science* (Washington, D.C.) **214**(4521), 660 (1981).
- K. Ugurbil, T. R. Brown, J. A. den Hollander, P. Glynn and R. G. Shulman, *Proc. Nat. Acad. Sci. USA* **75**, 3742 (1978).
- J. A. den Hollander, T. R. Brown, K. Ugurbil and R. G. Shulman, *Proc. Nat. Acad. Sci. USA* **76**, 6096 (1979).
- F. Lynen, *Symp. Soc. Gen. Physiol.* **8**, 289 (1961).
- L. H. Stickland, *Biochem. J.* **64**, 503 (1956).
- C. Gancedo, *J. Bacteriol.* **107**, 401 (1971).
- P. Tortora, M. Birtel, A.-G. Lenz and H. Holzer, *Biochem. Biophys. Res. Commun.* **100**, 688 (1981).
- D. J. Manners. The structure and biosynthesis of storage carbohydrates in yeast. In *The Yeasts* (Edited by A. H.

- Rose and J. S. Harrison), Vol. 2, pp. 419-439-439. Academic Press, New York (1971).
- <sup>19</sup>J. A. den Hollander, K. L. Behar and R. G. Shulman, *Proc. Nat. Acad. Sci. USA* **2693** (1981).
- <sup>20</sup>J. K. Barton, J. A. den Hollander, J. J. Hopfield and R. G. Shulman, *J. Bacteriol.* **151**, 177 (1982).
- <sup>21</sup>A. L. Lehninger, *Biochemistry*, pp. 446-467. Worth, New York (1975).
- <sup>22</sup>S. M. Cohen, S. Ogawa and R. G. Shulman, *Proc. Nat. Acad. Sci. USA* **76**, 1603 (1979).
- <sup>23</sup>S. M. Cohen, P. Glynn and R. G. Shulman, *Proc. Nat. Acad. Sci. USA* **78** 60 (1981).
- <sup>24</sup>S. M. Cohen, R. G. Shulman and A. C. McLaughlin, *Proc. Nat. Acad. Sci. USA* **76** 4808 (1979).
- <sup>25</sup>S. M. Cohen, R. G. Shulman, J. R. Williamson and A. C. McLaughlin, In *Alcohol and Aldehyde Metabolizing Systems IV* (Edited by R. G. Thurman). Plenum Press, New York (1980).
- <sup>26</sup>S. M. Cohen, R. Rognstad, R. G. Shulman and J. Katz, *J. Biol. Chem.* **256**, 3428 (1981).
- <sup>27</sup>J. J. Batenburg and M. S. Olson, *J. Biol. Chem.* **251**, 1364 (1976).
- <sup>28</sup>M. F. Utter and M. C. Scrutton, *Current Topics in Cellular Regulation*. (Edited by B. L. Horecker and E. R. Stadtman), Vol 1, pp. 253-296, Academic Press, New York (1969).